atmosphere

MDPI

Technical Note

Application of a Cloud Removal Algorithm for Snow-Covered Areas from Daily MODIS Imagery over Andes Mountains

Cristian Mattar [1,*], Rodrigo Fuster [2] and Tomás Perez [1]

[1] Laboratory of Geosciences (Geolab), University of Aysén, Calle Obispo Vielmo N° 62, Coyhaique 5952039, Chile; tomas.perez@uaysen.cl
[2] Department of Environmental Sciences and Renewable Natural Resources, Faculty of Agricultural Sciences, University of Chile, Avenida Santa Rosa N° 11315, Santiago 8820808, Chile; rfuster@uchile.cl
* Correspondence: cristian.mattar@uaysen.cl

Abstract: Snow cover area is dramatically decreasing across the Los Andes Mountains and the most relevant water reservoir under drought conditions. In this sense, monitoring of snow cover is key to analyzing the hydrologic balance in snowmelt-driven basins. MODIS Snow Cover daily products (MOD10A1 and MYD10A1) allow snow cover to be monitored at regular time intervals and in large areas, although the images often are affected by cloud cover. The main objective of this technical note is to evaluate the application of an algorithm to remove cloud cover in MODIS snow cover imagery in the Chilean Andes mountains. To this end, the northern region of Chile (Pulido river basin) during the period between December 2015 and December 2016 was selected. Results were validated against meteorological data from a ground station. The cloud removal algorithm allowed the overall cloud cover to be reduced from 26.56% to 7.69% in the study area and a snow cover mapping overall accuracy of 86.66% to be obtained. Finally, this work allows new cloud-free snow cover imagery to be produced for long term analysis and hydrologic models, reducing the lack of data and improving the daily regional snow mapping.

Keywords: Andes mountains; MODIS; snow cover; cloud removal

Citation: Mattar, C.; Fuster, R.; Perez, T. Application of a Cloud Removal Algorithm for Snow-Covered Areas from Daily MODIS Imagery over Andes Mountains. *Atmosphere* **2022**, *13*, 392. https://doi.org/10.3390/atmos13030392

Academic Editors: Małgorzata Falarz and Ewa Bednorz

Received: 16 November 2021
Accepted: 12 January 2022
Published: 26 February 2022

1. Introduction

Snow is an essential component of the climate system on the atmospheric processes, due to its high albedo, low thermal conductivity and considerable latent heat [1]. However, the snow is affected by climate change in most regions, decreasing the cover area due to positive feedback with the air temperature, especially during the spring and summer seasons [2,3]. In this sense, semiarid regions are highly sensitive to climate change in terms of the increase in air temperatures and the strong variability in distribution of precipitation, which forces snow to melt and affect the water balance, which in turn affects human activities [4]. Given the importance of snowmelt and its potential impact on water resources of snow-covered regions, the monitoring of snow is an important input to be obtained through the measurements of snow-covered area (SCA), snow depth (SD) and snow-water equivalent (SWE) [5]. However, ground-based snow monitoring and its properties can be very problematic in mountainous areas due to the rugged topography and adverse weather conditions [6]. For this reason, remote sensing is useful at providing information on snow cover areas in mountainous regions at regular intervals of time [7].

Remote sensing can assess snow cover by using Synthetic Aperture Radar (SAR), Light Detection and Ranging (LiDAR), passive optical technologies, among others [8]. The identification of SCA is mainly obtained from optical remote sensing data through the Normalized Difference of Snow Index (NDSI), due to its high reflectance in the green optical band and low reflectance in the near-infrared band being able to differentiate snow from other features [9–11]. Nevertheless, the NDSI is affected by cloudy conditions in the discrimination snow/clouds especially during snow accumulation periods when

clouds gather and obstruct the SCA [12,13]. Snow cover estimation methods in cloudiness scenes mainly consist of spatiotemporal filters to mitigate cloud cover such as the MODIS products [14–17]. A comprehensive review about cloud removal filters over agriculture and other areas is detailed in [18,19].

In the Andes mountains, snow cover started to be intensively monitored owing the impacts of climate change [20]. Indeed, several studies have documented a decrease in SCA and in snow cover duration (SCD). For instance, Prieto et al. [21] demonstrated a decrease in SCA and SCD between 1885 and 2000 in Mendoza, Argentina. Malmros et al. [22] found that SCA and SCD decreased by an average of ~13 $\pm$ 2% and 43 $\pm$ 20 days, respectively, over the 2000–2016 period in central the Chilean and Argentinean Andes. Stehr et al [23] studied snow cover over five Chilean Andean watersheds between the latitudes of 32.0 and 39.5° S, detecting an important decline in snow cover coincident with a deficit in precipitation. As well as identifying a significant decreasing trend in snow cover, they also found a snowline elevation at 10–30 m per year^{-1} at south of latitudes of 29–30° S, in addition to the impact of sublimation on arid mountains [24–26]. Pérez et al [25] studied Chilean Patagonia and identified a decreasing non-significant trend in annual mean SCA with a -20 km^2 per year^{-1} slope in the 2000–2016 period. These works used the 8-day MODIS composite product, which retrieves the maximum value of NDSI, neglecting the impact of daily SCA and affecting the SCD patterns. Thus, the objective of this paper is to apply a cloud removal algorithm for daily MODIS snow cover images in the Andes regions, specifically the Copiapó river basin, which is suffering a severe drought and limited water availability [27–31].

2. Study Area

The study area is the Pulido river basin located in the highest part of the Andes mountains in the Atacama region, Chile. The basin has an approximate area of 2100 km^2 that drains to the Pulido river, which is the main tributary of the Copiapó river basin. The climate is characterized by marginal high-altitude desert, where rainfall fluctuates around 250 mm, and in the upper mountainous part, there is solid precipitation. The presence of snow in this region allows the development of pluvio-nival feeding rivers, with permanent courses throughout the year of exoreic character [27]. Inside the basin, above 4000 m.a.s.l, is located La Ollita meteorological station (Figure 1) installed on December 2015, in the coordinates 28.20° S and 69.54° W.

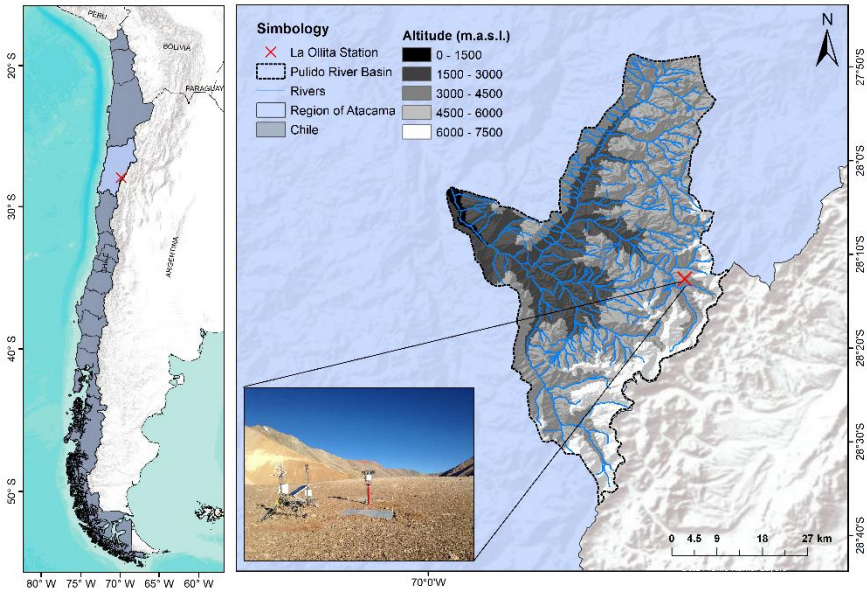

Figure 1. Study area of Pulido river basin and La Ollita site.

3. Data and Pre-Processing

3.1. Remote Sensing Data

The MODIS dataset used was daily snow cover products MOD10A1 (Terra) and MYD10A1 (Aqua) V6. Snow cover is identified using the NDSI at the spatial resolution of 500 m [32]. The original values of the MODIS product were classified into three classes: snow, no-snow (including water bodies) and clouds. The snow class corresponded to values greater than 0.4 according to the most common NDSI threshold to identify snow [9,33]. The values lower than or equal to 0.4 were associated with no-snow class.

3.2. Meteorological Data

A ground station (La Ollita) was used to compare and validate satellite imagery using meteorological instruments as well as SD and SWE. SD was measured using acoustic snow depth sensor (Campbell Scientific, SR50A) and SWE was measured using a Snow Scale (Sommer, SSG-2). Moreover, air temperature (Campbell, HC2S3) and soil temperature at 12 cm (Campbell, CS655) were included in the analysis. The time interval of measurements was set up at 30 min.

4. Methods

4.1. Cloud Removal Algorithm

To reduce the effects of clouds, the methodology proposed for [25] was adapted to the current version of the MODIS Snow Cover daily product on the Andes mountains. The first step is the combination of Terra and Aqua imagery that obtain the maximum value on a pixel basis by a class priority order (e.g., snow > no-snow > clouds) (1). The pixels classified as clouds in a Terra image are updated with an Aqua image of the same day when a pixel at the same location presents a snow or no-snow class pixel, or vice versa.

$$S^{C}_{(x,y,t)} = \mathbf{max}\left(S^{T}_{(x,y,t)}, S^{A}_{(x,y,t)}\right) \quad (1)$$

where y is the index for row (vertical); x is the index for column (horizontal) and t is the index for day of pixel S. S^{T} and S^{A} correspond to the Terra and Aqua pixels, respectively, and S^{C} to maximum of the combination between Terra and Aqua pixels.

The second step replaces cloud pixels in the S^{C} by the most recent preceding cloud-free observation at the same pixel. The backward temporal filter (BTF) is applied in one shift over snow-covered pixels (2) and then over no-snow pixels (3).

$$S^{TF}_{(x,y,t)} = \mathbf{S\ if}\left(S^{C}_{(x,y,t)} = C\ \textit{and}\ S^{C}_{(x,y,t-n)} = S\right) \quad (2)$$

$$S^{TF}_{(x,y,t)} = \mathbf{L\ if}\left(S^{C}_{(x,y,t)} = C\ \textit{and}\ S^{C}_{(x,y,t-n)} = L\right) \quad (3)$$

where S^{TF} is the backward temporal filter and n is the day of the temporal window (1, 2 and 3 days ago). C, L and S is for cloud cover, no-snow (land) and snow class, respectively.

4.2. Comparison and Validation of Cloud Removal Algorithm with Ground Data

The accuracy of the cloud removal algorithm over MODIS snow cover images was evaluated by using SD measurements (Table 1). Snow observations at the station are considered as ground truth for the pixel when SD > 0 cm in order to calculate the confusion matrix.

Table 1. Confusion matrix between MODIS cloud-free imagery and ground measurements.

		Ground Measurements (SD)	
		Snow (>0 cm)	No-Snow (≤0 cm)
MODIS	Snow	a	b
	No-snow	c	d

The overall accuracy (OA) is presented in Equation (4). Moreover, producer's accuracy (PA) and user's accuracy (UA) were also calculated.

$$OA = \frac{(a+d)}{(a+b+c+d)} * 100\% \quad (4)$$

5. Results

The cloud removal algorithm performance is shown in Figure 2. Terra has a cloud cover of 26.56%, while Aqua has a cloud cover of 28.49%. The combination of Terra and Aqua decreases cloud cover to 20.77%. The BTF with a time window of 1, 2 and 3 days decreases the cloud cover to 12.83%, 10.08% and 7.69%, respectively. Regarding to SCA, Terra presents 7.60% and Aqua 6.94%, and the combination of the two increases the SCA to 10.09%. The BTF with a time window of 1, 2 and 3 days increases the SCA to 12.04%, 12.96% and 13.63%, respectively.

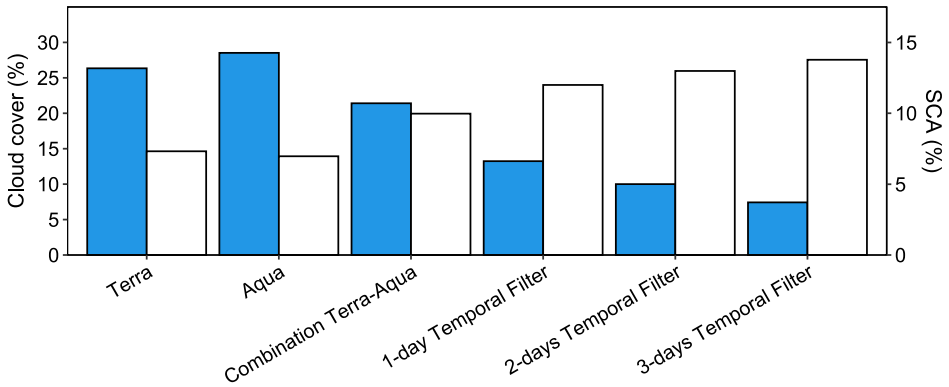

Figure 2. Performance of cloud removal algorithm for cloud (blue) and snow (white) classes for the period of 21 December 2015–21 December 2016.

Figure 3 shows the performance of the cloud removal algorithm for an image of 19 August 2016. The Terra image shows a cloud cover of 20.19% and the Aqua image a cloud cover of 48.51%. The combination of MODIS Terra and Aqua reduces the cloud cover to 19.73%. Finally, the image after the 3-day BTF is a cloud-free image.

The comparison between the MODIS imagery after the cloud removal algorithm and the in-situ data from La Ollita station is presented in Figure 4. The study site starts the snow accumulation in April 2016, which is coincident with a regular peak of SD and SWE. Between May and June 2016, there is a lack of snow cover mapping, due to a persistence of cloud cover over the station site. The snow cover season continues until October 2016 with a coincident maximum of SD and SWE at the beginning of September 2016 of 45.53 cm and 81.43 mm, respectively. Finally, in the middle of December 2016, a new maximum of SD and SWE values matching with a snow-covered pixel retrieved from the MODIS cloud removal algorithm. Moreover, the comparison with the air temperature shows a relationship between the snow-covered pixels and the decrease in the air temperature under zero degrees, which also coincides with the soil temperature in snow-covered days.

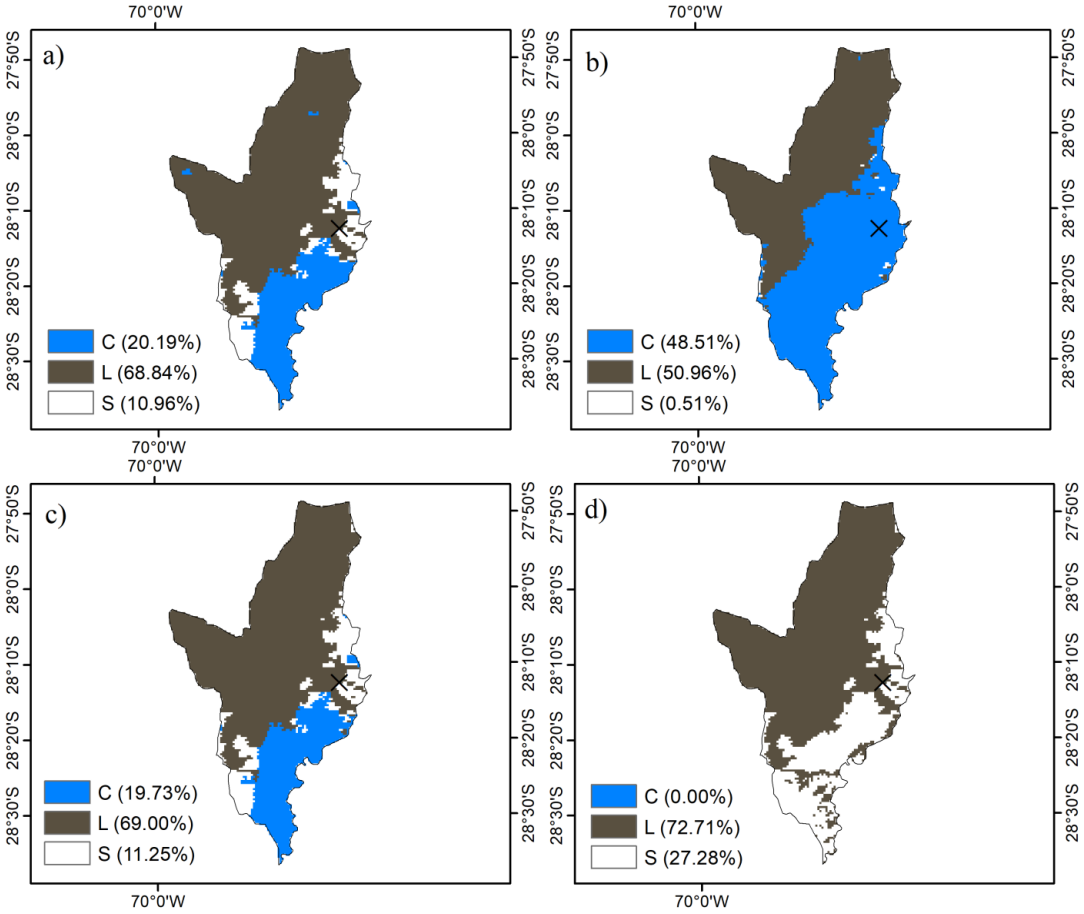

Figure 3. Cloud removal algorithm steps for MODIS image from 19 August 2016 (**a**) Terra, (**b**) Aqua, (**c**) Combination Terra–Aqua and (**d**) 3-day BTF. C, L and S is for cloud cover, no-snow (land) and snow class, respectively.

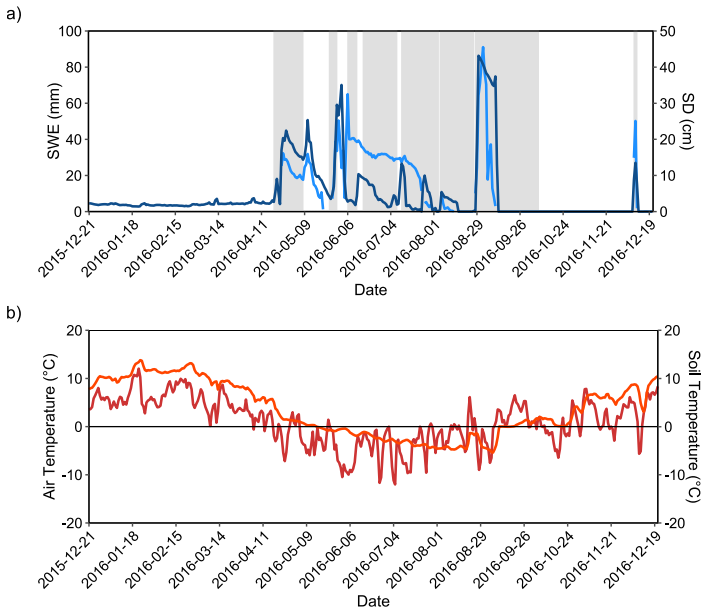

Figure 4. (**a**) Series of daily data of SD (brown) and SWE (blue) measured at the La Ollita station. In background, snow as grey; (**b**) Series of daily data of air and soil temperature as red and orange colour, respectively.

The validation of the cloud removal algorithm is presented in the Table 2 in the confusion matrix of the comparison between MODIS daily cloud-free images and SD measurements. The overall accuracy is 86.66% for the entire time period, correctly classifying 85 images at snow-covered pixels and 188 images as pixels without snow presence, matching the observation from the satellite with the ground measurement. The UA from the cloud removal algorithm in MODIS daily cloud-free images was 66.90% for the snow class and 83.90% for the no-snow class. On the other hand, the PA from the SD measurements station was 70.83% for the snow class and 96.40% for the no-snow class. Finally, 36 images were covered by clouds without retrieving a pixel where snow could be obtained, probably due to cloud persistence for more than 3 days of the BTF.

Table 2. Confusion matrix between modis cloud-free imagery and ground measurements.

		Ground Measurements (SD)		
		Snow (>0 cm)	No-Snow (≤0 cm)	UA (%)
MODIS	Snow	85	35	66.90
	No-snow	7	188	83.90
	PA (%)	70.83	96.40	
	OA (%)	86.66		

The MODIS snow cover cloud removal algorithm scaled to Chile is presented in the Figure 5 for an image of 12 August 2016. The Terra image has a cloud cover of 55.90%, while the Aqua image has a cloud cover of 54.98% and combining the two reduced cloud cover to 51.63%. However, the 3-day BTF decreased the cloud cover to 17.50%, where the remaining cloud cover is mainly centered in the austral region of Chile.

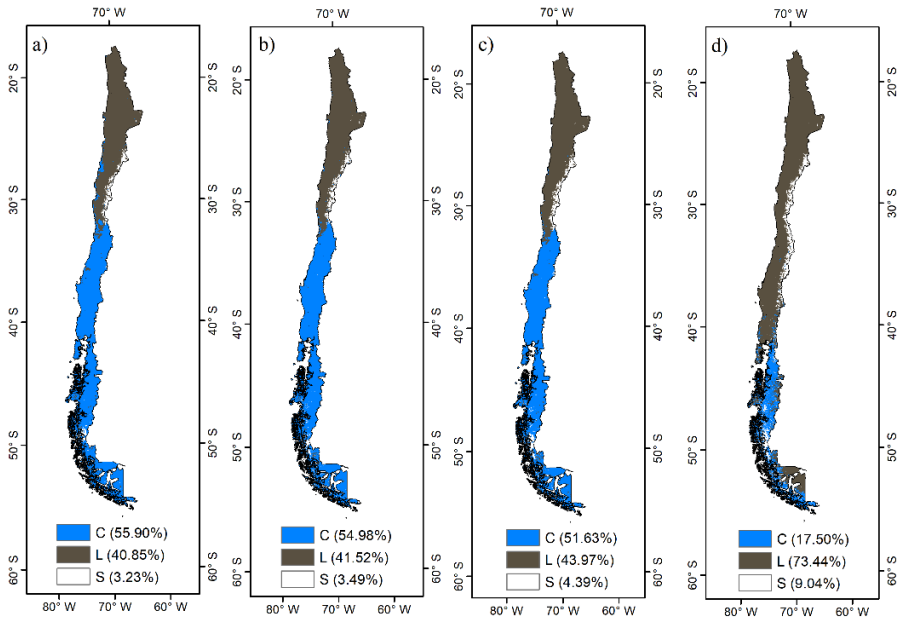

Figure 5. Cloud removal algorithm steps for MODIS image of 12 August 2016 (**a**) Terra, (**b**) Aqua, (**c**) Combination Terra-Aqua and (**d**) 3-days BTF.

The SCA daily maps generated at regional scale could be used for daily water balance retrievals to estimate river discharges and also to compare water regime in the framework of climate change scenarios. In this sense, it is necessary to implement instruments of SD and SWE in meteorological stations located in the Andes mountains, which commonly are located only in ski resorts, to validate of the algorithm in other latitudes.

6. Conclusions and Discussion

The cloud removal algorithm decreased the cloud cover in the Pulido river basin from 26.56% to 7.69% in the study area, where snow-covered regions are located over the higher parts of the Andes mountains.

In general terms, the MODIS snow cover product has good agreement with ground observations, with always over 90% accuracy when the sky is clear, mainly analyzed in studies of the Northern Hemisphere [34–38], but in the Chilean Andes, the mapping accuracy is more variable, due to the complex topography of the MODIS 8-day snow cover composites (MOD10A2) used in [23] in six basins of the central-southern region of Chile and achieved an overall accuracy of 81 to 98% with SCA compared with ground observations. In this study, the cloud removal algorithm generates a snow cover mapping accuracy close to 87% over the Pulido river basin, where the temporal resolution was improved at daily scale mostly suitable for hydrological modelling. Snow-false episodes were produced by the low spatial resolution of MODIS products and physiographic conditions (e.g., shadow effect). Finally, the contribution of a cloud removal algorithm consists of a daily application for the Andes mountains in Chile, decreasing the impact of a lack of snow cover information. In fact, the decrease in the cloud cover impact allows for an improvement in snow cover analysis and hydrologic models over snowmelt-driven basins.

Author Contributions: Conceptualization, T.P., C.M. and R.F.; methodology, T.P. and C.M.; software, T.P. and C.M.; validation, T.P., C.M. and R.F. formal analysis, T.P., C.M. and R.F.; investigation, T.P. and C.M.; data curation, T.P.; writing—original draft preparation, T.P., C.M. and R.F; writing—review and editing, T.P., C.M. and R.F; visualization, T.P.; funding acquisition, C.M. and R.F. All authors have read and agreed to the published version of the manuscript.

Funding: This research was funded by ANID FONDEF ID20I10034, Uchile-UPuente 2021–2022.

Institutional Review Board Statement: Not applicable.

Informed Consent Statement: Not applicable.

Data Availability Statement: The study did not report any data.

Acknowledgments: The authors are also grateful for open access to NASA products. We extend a special thanks to the anonymous reviewers for their useful comments on this.

Conflicts of Interest: The authors declare no conflict of interest.

References

1. Goodrich, L.E. The influence of snow cover on the ground thermal regime. *Can. Geotech. J.* **1982**, *19*, 421–432. [CrossRef]
2. Bates, B.C.; Kundzewicz, Z.W.; Wu, S.; Palutikof, J.P. *Climate Change and Water, Technical Paper VI of the Intergovernmental Panel on Climate Change*; IPCC Secretariat: Geneva, Switzerland, 2008; pp. 210–225.
3. Lemke, P.; Ren, J.; Alley, R.B.; Allison, I.; Carrasco, J.; Flato, G.; Fujii, Y.; Kaser, G.; Mote, P.; Thomas, R.H.; et al. Observations: Changes in Snow, Ice and Frozen Ground. In *Climate Change 2007: The Physical Science Basis. Contribution of Working Group I to the Fourth Assessment Report of the Intergovernmental Panel on Climate Change*; Cambridge University Press: Cambridge, UK, 2007.
4. Huang, J.; Guan, X.; Ji, F. Enhanced cold-season warming in semi-arid regions. *Atmos. Chem. Phys.* **2012**, *12*, 5391–5398. [CrossRef]
5. Kongoli, C.; Romanov, P.; Ferraro, R. 15 Snow Cover Monitoring. In *Remote Sensing of Drought: Innovative Monitoring Approaches*; CRC Press: Boca Raton, FL, USA, 2012; pp. 359–386.
6. Barnett, T.P.; Adam, J.C.; Lettenmaier, D.P. Potential impacts of a warming climate on water availability in snow-dominated regions. *Nature* **2005**, *438*, 303–309. [CrossRef] [PubMed]
7. Dietz, A.J.; Kuenzer, C.; Gessner, U.; Dech, S. Remote sensing of snow—A review of available methods. *Int. J. Remote Sens.* **2011**, *33*, 4094–4134. [CrossRef]
8. Painter, T.H.; Berisford, D.F.; Boardman, J.W.; Bormann, K.J.; Deems, J.; Gehrke, F.; Hedrick, A.; Joyce, M.; Laidlaw, R.; Marks, D.; et al. The Airborne Snow Observatory: Fusion of scanning lidar, imaging spectrometer, and physically-based modeling for mapping snow water equivalent and snow albedo. *Remote Sens. Environ.* **2016**, *184*, 139–152. [CrossRef]
9. Dozier, J. Spectral Signature of Alpine Snow Cover from the Landsat Thematic Mapper. *Remote Sens. Environ.* **1989**, *28*, 9–22. [CrossRef]
10. Hall, D.K.; Riggs, G.A.; Salomonson, V.V.; DiGirolamo, N.E.; Bayr, K.J. MODIS snow-cover products. *Remote Sens. Environ.* **2002**, *83*, 181–194. [CrossRef]
11. Hall, D.K.; Riggs, G.A. Accuracy assessment of the MODIS snow products. *Hydrol. Process.* **2007**, *21*, 1534–1547. [CrossRef]

12. Hüsler, F.; Jonas, T.; Riffler, M.; Musial, J.P.; Wunderle, S. A satellite-based snow cover climatology (1985–2011) for the European Alps derived from AVHRR data. *Cryosphere* **2014**, *8*, 73–90. [CrossRef]
13. Tran, H.; Nguyen, P.; Ombadi, M.; Hsu, K.-L.; Sorooshian, S.; Qing, X. A cloud-free MODIS snow cover dataset for the contiguous United States from 2000 to 2017. *Sci. Data* **2019**, *6*, 180300. [CrossRef]
14. Parajka, J.; Bloschl, G. Spatio-temporal combination of MODIS images—Potential for snow cover mapping. *Water Resour. Res.* **2008**, *44*, W03406. [CrossRef]
15. Gafurov, A.; Bárdossy, A. Cloud removal methodology from MODIS snow cover product. *Hydrol. Earth Syst. Sci.* **2009**, *13*, 1361–1373. [CrossRef]
16. Wang, X.; Xie, H.; Liang, T.; Huang, X. Comparison and validation of MODIS standard and new combination of Terra and Aqua snow cover products in northern Xinjiang, China. *Hydrol. Process.* **2009**, *23*, 419–429. [CrossRef]
17. Paudel, K.P.; Andersen, P. Monitoring snow cover variability in an agropastoral area in the Trans Himalayan region of Nepal using MODIS data with improved cloud removal methodology. *Remote Sens. Environ.* **2011**, *115*, 1234–1246. [CrossRef]
18. Li, X.; Wang, L.; Cheng, Q.; Wu, P.; Gan, W.; Fang, L. Cloud removal in remote sensing images using nonnegative matrix factorization and error correction. *ISPRS J. Photogramm. Remote Sens.* **2019**, *148*, 103–113. [CrossRef]
19. Chen, Y.; He, W.; Yokoya, N.; Huang, T.-Z. Blind cloud and cloud shadow removal of multitemporal images based on total variation regularized low-rank sparsity decomposition. *ISPRS J. Photogramm. Remote Sens.* **2019**, *157*, 93–107. [CrossRef]
20. Masiokas, M.H.; Villalba, R.; Luckman, B.H.; Le Quesne, C.; Aravena, J.C. Snowpack variations in the central Andes of Argentina and Chile, 1951–2005: Large-scale atmospheric influences and implications for water resources in the region. *J. Clim.* **2006**, *19*, 6334–6352. [CrossRef]
21. Prieto, R.; Herrera, R.; Doussel, P.; Gimeno, L.; Ribera, P.; García Herrera, R.; Hernández, E. Interannual oscillations and trend of snow occurrence in the Andes region since 1885. *Aust. Meteorol. Mag.* **2001**, *50*, 164.
22. Malmros, J.K.; Mernild, S.H.; Wilson, R.; Tagesson, T.; Fensholt, R. Snow cover and snow albedo changes in the central Andes of Chile and Argentina from daily MODIS observations (2000–2016). *Remote Sens. Environ.* **2018**, *209*, 240–252. [CrossRef]
23. Stehr, A.; Aguayo, M. Snow cover dynamics in Andean watersheds of Chile (32.0–39.5° S) during the years 2000–2016. *Hydrol. Earth Syst. Sci.* **2017**, *21*, 5111–5126. [CrossRef]
24. Saavedra, F.A.; Kampf, S.K.; Fassnacht, S.R.; Sibold, J.S. Changes in Andes snow cover from MODIS data, 2000–2016. *Cryosphere* **2018**, *12*, 1027–1046. [CrossRef]
25. Pérez, T.; Mattar, C.; Fuster, R. Decrease in snow cover over the Aysén river catchment in Patagonia, Chile. *Water* **2018**, *10*, 619. [CrossRef]
26. Cordero, R.R.; Asencio, V.; Feron, S.; Damiani, A.; Llanillo, P.J.; Sepulveda, E.; Jorquera, J.; Carrasco, J.; Casassa, G. Dry-Season Snow Cover Losses in the Andes (18–40° S) driven by Changes in Large-Scale Climate Modes. *Sci. Rep.* **2019**, *9*, 16945. [CrossRef] [PubMed]
27. Jara, F.; Lagos-Zúñiga, M.; Fuster, R.; Mattar, C.; McPhee, J. Snow Processes and Climate Sensitivity in an Arid Mountain Region, Northern Chile. *Atmosphere* **2021**, *12*, 520. [CrossRef]
28. Olivera-Guerra, L.; Mattar, C.; Merlin, O.; Durán-Alarcón, C.; Artigas, A.S.; Fuster, R. An operational method for the disaggregation of land surface temperature to estimate actual evapotranspiration in the arid region of Chile. *ISPRS J. Photogramm. Remote Sens.* **2017**, *128*, 170–181. [CrossRef]
29. Rojas, L.A.R.; Moletto-Lobos, I.; Corradini, F.; Mattar, C.; Fuster, R.; Escobar-Avaria, C. Determining Actual Evapotranspiration Based on Machine Learning and Sinusoidal Approaches Applied to Thermal High-Resolution Remote Sensing Imagery in a Semi-Arid Ecosystem. *Remote Sens.* **2021**, *13*, 4105. [CrossRef]
30. Bitran, E.; Rivera, P.; Villena, M.J. Water management problems in the Copiapó Basin, Chile: Markets, severe scarcity and the regulator. *Hydrol. Res.* **2014**, *16*, 844–863. [CrossRef]
31. Dirección General de Aguas (DGA). Diagnóstico y clasificación de los cursos y cuerpos de agua según objetivos de calidad Cuenca. In *Cuenca del río Copiapó*; DGA: Santiago, Chile, 2004.
32. Riggs, G.A.; Dorothy, K.H.; Román, M.O. *MODIS Snow Products Collection 6 User Guide*; National Snow & Ice Data Center: Boulder, CO, USA, 2015.
33. Hall, D.K.; Riggs, G.A.; Kääb, A.; Kumar, R.; Lawson, W.; Dobhal, D.P.; Stokes, C.R. Normalized-difference snow index (NDSI). In *Encyclopedia of Snow, Ice and Glaciers*; Springer: Dordrecht, The Netherlands, 2011; pp. 779–780.
34. Parajka, J.; Holko, L.; Kostka, Z.; Blöschl, G. MODIS snow cover mapping accuracy in a small mountain catchment—Comparison between open and forest sites. *Hydrol. Earth Syst. Sci.* **2012**, *16*, 2365–2377. [CrossRef]
35. Liang, T.G.; Huang, X.D.; Wu, C.X.; Liu, X.Y.; Li, W.L.; Guo, Z.G.; Ren, J.Z. An application of MODIS data to snow cover monitoring in a pastoral area: A case study in Northern Xinjiang, China. *Remote Sens. Environ.* **2008**, *112*, 1514–1526. [CrossRef]
36. Huang, X.; Liang, T.; Zhang, X.; Guo, Z. Validation of MODIS snow cover products using Landsat and ground measurements during the 2001–2005 snow seasons over northern Xinjiang, China. *Int. J. Remote Sens.* **2011**, *32*, 133–152. [CrossRef]
37. Muhammad, S.; Thapa, A. Daily Terra–Aqua MODIS cloud-free snow and Randolph Glacier Inventory 6.0 combined product (MOD10A1GL06) for high-mountain Asia between 2002 and 2019. *Earth Syst. Sci. Data* **2021**, *13*, 767–776. [CrossRef]
38. Muhammad, S.; Thapa, A. An improved Terra–Aqua MODIS snow cover and Randolph Glacier Inventory 6.0 combined product (MOYDGL06*) for high-mountain Asia between 2002 and 2018. *Earth Syst. Sci. Data* **2020**, *12*, 345–356. [CrossRef]